Developmental Biology 339 (2010) 1–13

Contents lists available at ScienceDirect

Developmental Biology

journal homepage: www.elsevier.com/developmentalbiology

The *Drosophila* LEM-domain protein MAN1 antagonizes BMP signaling at the neuromuscular junction and the wing crossveins

Nicole Wagner [a,b,*], Annika Weyhersmüller [c], Anna Blauth [d], Tamara Schuhmann [d], Manfred Heckmann [b], Georg Krohne [d], Christos Samakovlis [a,*]

[a] Department of Developmental Biology, Wenner-Gren Institute, Stockholm University, S-10691 Stockholm, Sweden
[b] Department of Physiology–Neurophysiology, Institute of Physiology, University of Wuerzburg, D-97070 Wuerzburg, Germany
[c] Carl-Ludwig-Institute for Physiology, University Leipzig, D-04103 Leipzig, Germany
[d] Division of Electron Microscopy, Biocenter of the University of Wuerzburg, D-97074 Wuerzburg, Germany

ARTICLE INFO

Article history:
Received for publication 20 October 2009
Revised 17 November 2009
Accepted 19 November 2009
Available online 28 December 2009

Keywords:
MAN1
LEM-domain protein
Inner nuclear membrane
BMP signaling
Mad
Drosophila
Neuromuscular junction
Crossvein
Pupal wing

ABSTRACT

BMP signaling responses are refined by distinct secreted and intracellular antagonists in different cellular and temporal contexts. Here, we show that the nuclear LEM-domain protein MAN1 is a tissue-specific antagonist of BMP signaling in *Drosophila*. MAN1 contains two potential Mad-binding sites. We generated $MAN1^{\Delta C}$ mutants, harbouring a MAN1 protein that lacks part of the C-terminus including the RNA recognition motif, a putative Mad-binding domain. $MAN1^{\Delta C}$ mutants show wing crossvein (CV) patterning defects but no detectable alterations in nuclear morphology. $MAN1^{\Delta C}$ pupal wings display expanded phospho-Mad (pMad) accumulation and ectopic expression of the BMP-responsive gene crossveinless-2 (cv-2) indicating that MAN1 restricts BMP signaling. Conversely, MAN1 overexpression in wing imaginal discs inhibited crossvein development and BMP signaling responses. *MAN1* is expressed at high levels in pupal wing veins and can be activated in intervein regions by ectopic BMP signaling. The specific upregulation of *MAN1* in pupal wing veins may thus represent a negative feedback circuit that limits BMP signaling during CV formation. $MAN1^{\Delta C}$ flies also show reduced locomotor activity, and electrophysiology recordings in $MAN1^{\Delta C}$ larvae uncover a new presynaptic role of MAN1 at the neuromuscular junction (NMJ). Genetic interaction experiments suggest that MAN1 is a BMP signaling antagonist both at the NMJ and during CV formation.

Introduction

Bone morphogenic proteins (BMPs) constitute a subfamily of the transforming growth factor β (TGF-β) gene family and play critical roles in animal development. The ligands, receptors and intracellular effectors are conserved from *Drosophila* to mammals (Raftery and Sutherland, 1999). Decapentaplegic (Dpp) and Glass-bottom-boat (Gbb) are two of the *Drosophila* BMPs (Arora et al., 1994; Haerry et al., 1998; Khalsa et al., 1998). They signal as homo- or heterodimers by stimulating the formation of heteromeric complexes of serine/threonine kinase receptors. These receptors include the type II receptor Punt or Wishful thinking (Wit), which upon ligand binding phosphorylates the type I receptors, Saxophone (Sax) and Thickveins (Tkv) (reviewed by O'Connor et al., 2006). The signal is propagated by phosphorylation of the transcription factor, Mothers against decapentaplegic (Mad), the sole receptor-activated Smad in *Drosophila* involved in BMP signaling (Sekelsky et al., 1995). Phosphorylated Mad (pMad) associates with the mediator Smad, Medea (Med). Once in the nucleus, the complex binds to DNA and activates or represses target genes depending on the presence of additional transcription factors.

Dpp functions in many developmental processes, and has several crucial roles during the formation of the adult wing (Affolter and Basler, 2007). The *Drosophila* wing is made of two apposed dorsal and ventral epithelial sheets, forming a stereotyped array of five longitudinal veins (LVs) and two crossveins (CVs). The determination and differentiation of vein patterns occurs during larval and pupal development and rely on at least five different conserved signaling pathways, including that of BMPs. Unlike the complex signaling interactions required for LV patterning, CV patterning is mostly dependent on Dpp- and Gbb-mediated BMP signaling during pupal development (Blair, 2007; Conley et al., 2000; Ray and Wharton, 2001; Ralston and Blair, 2005). Manipulations inhibiting BMP signaling during this phase affect the formation of the CVs, often with minimal effects on LV specification (Conley et al., 2000; Khalsa et al., 1998; Ray and Wharton, 2001). During CV formation in pupal wings, Dpp is expressed in LVs, while Gbb is expressed in the entire wing blade (Ralston and Blair, 2005). The extracellular proteins Short

* Corresponding authors. N. Wagner is to be contacted at fax: +49 931 318 2741. C. Samakovlis, fax: +46 8 6126127.
E-mail addresses: nicole.wagner@uni-wuerzburg.de (N. Wagner), christos@devbio.su.se (C. Samakovlis).

0012-1606/$ – see front matter © 2009 Elsevier Inc. All rights reserved.
doi:10.1016/j.ydbio.2009.11.036

gastrulation (Sog) and Crossveinless (Cv), a Twisted gastrulation (Tsg) homolog, bind to BMPs and mediate their transport to the presumptive CV region. The metalloprotease Tolloid-related (Tlr) cleaves Sog and allows ligand binding to the receptor (Marques et al., 1997; Serpe et al., 2005). Thereby Dpp/Gbb dimers from the LVs activate signaling in the prospective CV regions (Shimmi et al., 2005a, b). pMad first appears in a broad region at the site of the presumptive CVs and later refines to a narrow stripe. Posterior crossvein (PCV) patterning by BMP signaling involves additional proteins, including the secreted BMP-binding protein crossveinless 2 (cv-2), the kinase Nemo (Nmo), and the transmembrane protein Kekkon5 (Kek5) (Conley et al., 2000; Evans et al., 2009; Shimmi et al., 2005a; Vilmos et al., 2005; Zeng et al., 2007). cv-2 forms transient complexes with the ligands Dpp/Gbb and the Tkv receptor promoting or inhibiting signaling depending on its concentration and the composition of the ligand dimers (Serpe et al., 2008).

Gbb signaling has a prominent role at the *Drosophila* neuromuscular junction (NMJ), where it has been implicated in synaptic growth and maturation, baseline neurotransmission and synaptic plasticity as well as synaptic homeostasis (Aberle et al., 2002; Eaton and Davis, 2005; Haghighi et al., 2003; Marques et al., 2002; McCabe et al., 2004, 2003; Rawson et al., 2003; Sweeney and Davis, 2002). Neurons and muscles communicate through signals that coordinate the development of pre- and postsynaptic terminals. Anterograde signaling (neuron to muscle) defines various properties of the postsynapse, while retrograde signaling (muscle to neuron) influences synaptic growth, maturation, synaptic plasticity and homeostasis (Collins and DiAntonio, 2007). Retrograde BMP signaling at the NMJ is mediated by the release of Gbb from the muscle. Gbb signals to the presynaptic type II receptor Wit and Sax or Tkv. The signal is transduced via phosphorylation of presynaptic Mad. Together with Medea, pMad modulates the expression of unknown BMP-responsive target genes in the nucleus. An additional postsynaptic BMP signaling event has been described at the larval NMJ that is consistent with anterograde BMP signaling. Mad phosphorylation also occurs in regions facing the presynaptic active zone of neurotransmitter release (Dudu et al., 2006). The presence of multiple BMP dependent signaling events at the NMJ makes it a sensitive but complex model system for the analysis of novel BMP regulators.

The nuclear envelope segregates the nuclear and cytoplasmic activities in eukaryotic cells. It is composed of an inner and an outer membrane and perforated by nuclear pores. A network of lamin filaments and associated lamin-binding proteins at the inner nuclear membrane constitutes the nuclear lamina in multicellular organisms. The LEM-domain proteins are a subgroup of inner nuclear membrane (INM) proteins that share a common motif of 43 amino acids, known as LEM-domain. Mutations in the LEM-domain genes *LAP2*, *emerin* and *MAN1* are associated with a wide range of human diseases, including muscular dystrophies, neuropathies, cardiomyopathies, and bone and connective tissue disorders. Recent genetic evidence has suggested specific roles for LEM-proteins in BMP signaling. *Drosophila* Otefin binds to Medea and controls gene expression and stem cell behavior in the female germline (Jiang et al., 2008). In contrast to otefin, vertebrate MAN1 binds to Mad and pMad via its conserved C-terminal RRM motif (Bengtsson, 2007). The consequences of (partial) loss of *MAN1* differ in the analyzed model organisms, possibly reflecting specific and context-dependent roles of MAN1. In *Xenopus*, MAN1 regulates dorsoventral axis determination by antagonizing BMP signaling (Osada et al., 2003; Raju et al., 2003), whereas MAN1 is essential for embryonic vasculogenesis in mice where it modulates extracellular matrix deposition by the activity of TGF-β and Nodal signaling (Cohen et al., 2007; Ishimura et al., 2006, 2008). Also flies lacking MAN1 show aberrant wing venation, consistent with a possible antagonistic role of MAN1 in BMP signaling (Pinto et al., 2008). A previous yeast two-hybrid analysis suggests that Mad binds to the RRM-domain of MAN1 (Pinto et al., 2008) but this putative interaction has not been proven with an independent method. Heterozygous loss-of-function mutations in the human *MAN1* (*LEMD3*) gene are associated with Buschke–Ollendorff syndrome and Osteopoikilosis. The pathology of these diseases was attributed to increased bone density due to aberrant BMP/TGF-β signaling (Hellemans et al., 2004, 2006; Kawamura et al., 2005). Analysis of the mutant *LEMD3* alleles revealed that these alleles produce truncated forms of the MAN1 protein. The truncated forms lack the C-terminal RRM motif that interacts with receptor-activated Smads (R-Smads) in vitro and the phenotypes were proposed to be associated with increased BMP/TGF-β signaling (Osada et al., 2003; Raju et al., 2003, Lin et al., 2005; Pan et al., 2005). To separate the potential roles of MAN1 in NE formation and integrity from its function in BMP signaling, we generated $MAN1^{\Delta C}$ mutants expressing a MAN1 protein lacking the C-terminal Mad-binding domain at endogenous levels. Here, we present the analysis of BMP signaling during crossvein development in $MAN1^{\Delta C}$ flies and we describe a new role of MAN1 in NMJ function. The analysis shows that BMP signaling is expanded in $MAN1^{\Delta C}$ mutants. MAN1 expression is upregulated in the vein regions of wildtype pupal wings and can be induced in intervein regions by Gbb overexpression. We found that MAN1 binds to Mad in vivo and in vitro and MAN1 overexpression studies suggest an antagonistic role of MAN1 in a subset of BMP signaling events.

Materials and methods

Drosophila strains

Flies were raised on standard medium at 25 °C. The following fly strains were used: w^{1118}, *actin5C*GAL4, *elav*GAL4, *mef2*GAL4, *MS1096*GAL4, *engrailed*GAL4, dpp^{S11} (Bloomington) and gbb^{1} (kindly provided by S. Thor). To generate alleles of *MAN1*, the P-element insertion KG06361 (Bloomington) was mobilized to generate imprecise excisions. The molecular structure of the *MAN1* excision alleles was analyzed by polymerase chain reaction and sequencing. The deletion found in $MAN1^{\Delta C}$ is limited to the *Drosophila* MAN1 gene. It starts at position +1437 relative to the transcription start site and extends to +2117, with 321 bp of the P-element remaining at the initial insertion site, leaving the neighbouring gene CG13567 unaffected. The following primers were used for sequencing: 5′-primer (2R:19921234..19925254): GACTCACAGGGGAAATCTGCA; 3′-primer (2R:19923291..19927314): CTTAGGCGCACATTTGCATACATC. To generate MAN1 rescue constructs, the protein-coding region of *MAN1* was amplified from a cDNA library and cloned into pUAST, which was injected into embryos to obtain stable transformant lines. Although we did not include any regulatory sequence in the UASMAN1 construct, each of the obtained 17 transgenic lines showed comparable leaky expression of the transgene. For the analysis of genetic interactions, $w;MAN1^{\Delta C}/CyOtwistGFP$ flies were recombined with flies of the genotypes $w;dpp^{S11}/CyO$ or $w;gbb^{1}/CyO$ and positively tested recombinants were then crossed to $w;MAN1^{\Delta C}/CyOtwistGFP$ to obtain $w;MAN1^{\Delta C};dpp^{S11}/MAN1^{\Delta C}$ and $MAN1^{\Delta C};gbb^{1}/MAN1^{\Delta C}$ mutant flies.

Immunohistochemistry, SDS-PAGE and immunoblotting

For antibody staining of embryos, body wall preparations, muscle fibers, imaginal disks, salivary glands, gut, fat body and trachea, the dissected specimens or embryos were fixed in 4% formaldehyde for 20 min, followed by three 5 min washes in PBS followed by 15 min permeabilization in PBT (0.1% Triton X-100 in PBS). Prior to overnight incubation with primary antibodies, embryos or tissues were blocked in PBS, 0.1% BSA for 1 h. For antibody staining of pupal wings, white prepupae were selected and aged as appropriate, then dissected in PBS and fixed in 4% formaldehyde in PBT overnight at 4 °C. Fixed preparations were rinsed in PBT and the pupal cuticle was removed from the wings. Wings were incubated for 1 h in PBT, 0.1% BSA.

Specimens were incubated with primary antibodies (diluted in PBT, 0.1% BSA) overnight at 4 °C or 1 h at room temperature with FITC conjugated phalloidin (1:50; SIGMA). Samples were washed four times in PBT–0.1% BSA. Secondary antibodies were diluted in PBT–0.1% BSA and samples incubated for 2h at room temperature. Preparations were washed four times with PBT, two times with PBS, mounted in Vectashield (Vector Laboratories) or 70% glycerine in PBS and imaged on a Zeiss LSM510 confocal microscope. Primary antibodies: (polyclonal, anti-guinea pig: MAN1, 1:500; lamin Dm0, 1:1000; otefin, 1:1000; dLBR, 1:1000; for details see Wagner et al., 2004, 2006); Tpr (polyclonal, anti-rabbit: 1:100; kindly provided by Volker Cordes), pMad (polyclonal, anti-rabbit: 1:3000; kindly provided by Carl-Henrik Heldin); DSRF (polyclonal anti-rat: 1:1000; kindly provided by Markus Affolter); mAb 22C10 (1:100; DSHB); mAb DiscLarge (1:100; DSHB); mAb Fasciclin II (1:100; DSHB); Synaptotagmin (1:100; DSHB); Bruchpilot (1:100; kindly provided by Erich Buchner); or FITC conjugated phalloidin (1:50; SIGMA). Secondary antibodies conjugated to Cy2 or Cy3 (Jackson Immunochemicals) or Alexa Fluor-488 (Molecular Probes) were used at 1:400 dilution. For SDS-PAGE and immunoblotting see Wagner et al. (2006).

In situ hybridization of pupal wings and wing handling of adult wings

In situ hybridization was performed as described (http://superfly.ucsd.edu/bierlab/research/protocols/imagdisc.html). Probes were digoxigenin-labeled single-stranded RNA from either the *MAN1* or *cv-2* open reading frame. Adult wings were dissected and rinsed in isopropanol followed by mounting in 70% glycerine in PBS.

Negative geotaxis assay

Ten flies of each genotype and age were placed into a vertical cylinder, tapped to the bottom, and given 20 s to climb a distance of 10 cm. Flies that successfully climbed 10 cm in 20 s were scored as positive. Each fly was tested a total of five times.

Electrophysiology

Two-electrode voltage clamp (TEVC) recordings were performed on ventral longitudinal muscle 6 of male third instar larvae in extracellular haemolymph-like solution HL3 containing 70 mM NaCl, 5 mM KCl, 20 mM $CaCl_2$, 10 mM $NaHCO_3$, 5 mM trehalose, 115 mM sucrose, 5 mM HEPES and 1 mM$CaCl_2$. Recordings were made from cells with initial membrane potentials between −50 and −70 mV and input resistances of at least 4 MΩ using intracellular electrodes with resistances of 10–35 MΩ filled with 3 M KCl. The holding potential was −60 mV for evoked excitatory postsynaptic currents (eEPSCs) and −80 mV for miniature excitatory postsynaptic currents (mEPSCs). EPSCs were recorded at 0.2 Hz. High-frequency stimulation protocols consisted of 100 pulses at 60 Hz. Care was taken to ensure the recruitment of both motoneurons innervating muscle 6. Recordings were analyzed with pClamp10 (Axon Instruments). For the analysis of genetic interaction of *MAN1* and *gbb*, eEPSCs of *w;MAN1*$^{\Delta C}$ mutants was compared to that of *w;gbb*^{1}*;/CyO* and *MAN1*$^{\Delta C}$*;gbb*^{1}*/MAN1*$^{\Delta C}$ mutants.

Co-immunoprecipitations and GST pull-down assays

For co-immunoprecipitation experiments, anti-MAN1 or anti-dLBR antibodies were bound to protein A Sepharose beads (Pharmacia Biotech, Sweden) for 2 h at room temperature under rotation in 100 µl PBS. Beads were washed twice with Na borate buffer (0.2 M Na borate, pH 9.0) and incubated in Na borate buffer containing 20 mM dimethyl pimelimidate (DMP) for 30 min at room temperature. DMP cross-linking was stopped by several washes of the beads in 0.2 M ethanolamine (pH 8.0) for 2 h at room temperature. Beads were washed two times in PBS and 2 times in immunoprecipitation (IP) buffer (1% Triton X-100, 150 mM NaCl, 20 mM Tris–HCl, 1 mM PMSF, 1 mM complete protease inhibitor (Roche), pH 7.4). Protein extracts from adult flies (100 flies/immunoprecipitation) were homogenized in 2 ml IP buffer, incubated for 20 min at 4 °C under rotation and cleared by repeated centrifugation at 13,000 g for 15 min at 4 °C. The cleared protein extract was preabsorbed to 10 µg of protein A Sepharose beads. The antibody-coupled beads were washed three times with PBS and two times with IP buffer and incubated with the cleared protein extract for 2 h at 4 °C under rotation. Beads were washed three times with IP buffer and two times with PBS. The resulting bead-bound immunocomplexes were analyzed by SDS-PAGE and immunoblotting according to standard techniques (Wagner et al., 2006).

In glutathione-S-transferase (GST) pull-down assays, Medea or MAN1 GST fusion proteins were expressed using pGEX 4T-1 in *E. coli* Rosetta cells and isolated with glutathione agarose (Lang and Krohne, 2003). GST fusion proteins were extracted by sonication in chilled TPE-lysis buffer (1% Triton X-100, 100 mM EDTA in PBS, pH 7.5). Cell debris were pelleted by centrifugation and the supernatant was bound to glutathione-agarose beads in PBS by end-over-end rotation for 15 h at 4 °C. After washing the beads three times with PBS and three times with wash buffer (1% Triton X-100, 10 mM methionine in PBS, pH 7.5), in vitro synthesized and ^{35}S-methionine labeled proteins were added, followed by another end-over-end rotation for 4 h at 4 °C. The beads were then pelleted through 30% sucrose, washed 3 times with 0.1% Triton X-100 in PBS and prepared for SDS-PAGE and autoradiography. Mad or MAN1 was in vitro synthesized and ^{35}S-methionine labeled using the TNT Coupled Reticulocyte Lysate System (Promega) and incubated with GST fusion proteins of MAN1 or Medea. Bound Mad or MAN1 was detected by autoradiography.

Image processing analysis

Image processing for confocal imaging was performed with Zeiss LSM510 software (Carl Zeiss MicroImaging, Inc.). Wide-field images of in situ hybridizations were acquired with Openlab version 3.1.4 (Improvision). Fluorescence-labeling and digoxigenin-labeling mean intensities were quantified from gray-scale images using ImageJ 1.41. The mean intensity is defined in ImageJ as the sum of gray values of all the pixels in the selection divided by the number of pixels and intensity scores ranged from 0 (black) to 255 (white). All images within an experiment were acquired under identical optical settings to enable comparisons of the mean pixel value. Immunofluorescence values were compared using Student's *t* test.

Statistical analysis

Tests for statistical significance were carried out using chi square test, Student's *t* test, ANOVA and Kaplan-Meier survival analysis (log-rank test). Data analysis which produced $p<0.05$ was accepted as statistically significant. Error bars indicated SEM.

Results

MAN1 interacts with Mad via two distinct binding sites

Previous yeast two-hybrid studies suggested that *Drosophila* MAN1 binds to Mad with its C-terminal domain (Pinto et al., 2008). To address if MAN1 binds to phosphorylated Mad we carried out co-immunoprecipitation experiments using a specific antibody against MAN1 and extracts from adult wildtype flies. MAN1 was found in complex with pMad suggesting that the two proteins associate with each other at endogenous levels *in vivo* (Fig. 1A). Parallel co-immunoprecipitations with antibodies against LBR, another lamin-

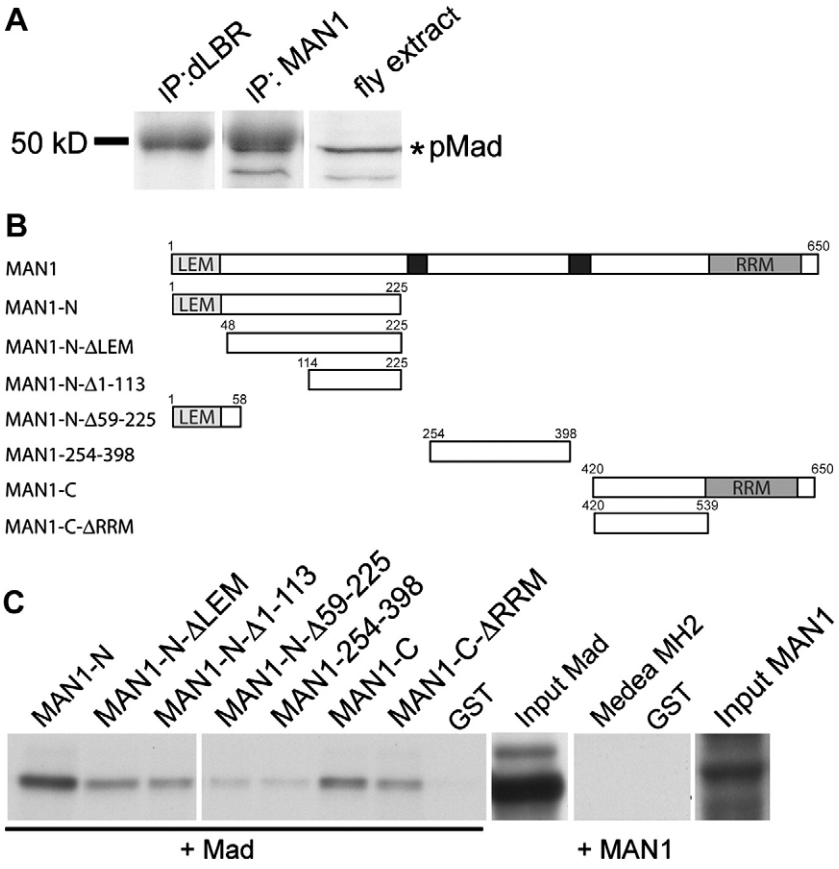

Fig. 1. MAN1 physically interacts with Mad via two distinct binding sites. (A) Co-immunoprecipitation of endogenous MAN1 and pMad from adult fly extracts. Immunoprecipitation was performed with polyclonal antibodies specific for MAN1 bound to protein A-Sepharose. As control, immunoprecipitation was performed with antibodies specific for LBR. Precipitated proteins were separated by SDS-PAGE and immunoblotted with rabbit polyclonal antibodies specific for pMad. Immunoblot showing endogenous levels of pMad in the fly extracts used for co-immunoprecipitation. The band at 50 kDa represents the antibody heavy chains of the antibodies used for the co-immunoprecipitation. (B) Schemes of GST-MAN1 fusion proteins used in the GST pull-down assay. Numbers mark the positions of individual amino acids. Boxes depict transmembrane domains (black), LEM-domain (LEM) and RRM. (C) Binding of GST-MAN1 fusion proteins to Mad and Binding of GST-Medea MH2 domain to MAN1. GST-MAN1 or GST-Medea fusion proteins were expressed from *E. coli* and incubated with ^{35}S-methionine labeled, in vitro synthesized Mad or MAN1. GST-MAN1 fusion proteins were pulled down using glutathione sepharose beads and bound proteins were analyzed by autoradiography of SDS-polyacrylamide gels. As an input control, audiograms show 10% of the ^{35}S-labelled Mad or MAN1 used in each binding reaction. Representative autoradiograms are shown from one of three independent experiments.

associated protein did not detect any interaction between LBR and pMad arguing that MAN1 binds specifically to pMad.

To assess if MAN1 and Mad bind to each other directly and map the binding domains, we performed glutathione-S-transferase (GST) pull-down assays using different truncations of MAN1 fused to GST. In these assays, ^{35}S-methionine labeled Mad was incubated with various truncated GST fusion proteins of MAN1 produced in Fig. 1B. In parallel assays we tested if the MH2 domain of Medea could bind to MAN1 (Fig. 1C). Consistent with our co-immunoprecipitation results, we found that MAN1 could bind Mad. In contrast, we detected no apparent association between MAN1 and Medea (Fig. 1C). The amounts of MAN-GST fusion proteins used in these assays were quantified by Coomassie blue staining (Fig. S1A and B″). The binding of MAN1-GST fusion proteins was quantified and illustrated as histograms (Fig. S1A′ and B′). Whereas GST alone or a GST-MAN1 fusion protein containing the central domain of MAN1 (amino acids 254–398) showed negligible pull-down activity, the C-terminal fusion of MAN1 (MAN1-C) was able to pull-down radiolabeled Mad. This binding was significantly reduced when we deleted the RRM domain (MAN1-C-ΔRRM), demonstrating that the RRM domain is important for the interaction of MAN1-C and Mad. Surprisingly, we also found that the N-terminal part of MAN1 (MAN1-N) was able to bind Mad with high affinity suggesting the presence of a second Mad-binding site, at least in vitro. All further truncations of MAN1-N (MAN1-N-ΔLEM, MAN1-N-Δ1-113) reduced Mad binding, and the lowest binding affinity exhibited the LEM-domain (MAN1-N-Δ59-225) and the segment in between the two membrane spanning domains (MAN1-254-398). Our data indicate that more than one protein segment of MAN1-N is involved in Mad binding. We suggest that interactions between weak binding (MAN1-N-Δ59-225) and stronger binding segments (MAN1-N-ΔLEM) could enhance Mad interaction of the N-terminal MAN1 domain. To rule out the possibility that the truncated N-terminal MAN1 fusions exhibit unspecific binding, we tested their ability to interact with Barrier-to-Autointegration Factor (BAF), a small chromatin-binding protein known to interact specifically with the LEM-domain (Wagner and Krohne, 2007). Only the two MAN1 constructs containing the LEM-domain (MAN1-N, MAN1-N-Δ59-225) showed significant binding to BAF. MAN1-N-ΔLEM did not bind to BAF suggesting that its association with Mad is specific (Fig. S1B and B′).

Generation and characterization of MAN1-deficient strains

Analysis of the defects caused by MAN1 inactivation in animals has been performed in worms (Liu et al., 2003), frogs (Osada et al., 2003; Raju et al., 2003), mice (Ishimura et al., 2006, 2008; Cohen et al., 2007), and flies (Pinto et al., 2008). The phenotypes of partial inactivation or complete loss of *MAN1* in these model organisms differ, possibly reflecting different molecular functions of MAN1. *Drosophila* mutants lacking MAN1 show wing-patterning phenotypes, consistent with a possible role of MAN1 in BMP signaling. However, we still lack molecular evidence for the antagonistic roles

of MAN1 in BMP signaling in flies (Pinto et al., 2008). To obtain further insight into *MAN1* functions in fly development and to further investigate the postulated specific role of MAN1 in BMP signaling, we generated new *MAN1* fly strains by imprecise P-element excision. The KG06361 strain carries a P element insertion that is located at the 3′end of the *MAN1* gene (Fig. 2A). We mobilized this P element to generate small deletions into the gene. We identified MAN1 mutants lacking any detectable MAN1 protein (Fig. S2A) and $MAN1^{\Delta C}$ mutants, expressing a MAN1 protein devoid of the C-terminal RRM domain (Fig. 2). The exact deletion endpoints in the $MAN1^{\Delta C}$ mutants were determined by sequencing of genomic DNA. The expected polypeptide expressed in $MAN1^{\Delta C}$ mutants extends to amino acid 480 and lacks the MAN1 C-terminus including the putative Smad-binding RRM domain (Fig. 2B). Western blots with an antibody against MAN1 recognized the full-length protein of ~72 kDa in lysates prepared from wildtype and $MAN1^{\Delta C}/+$ flies. We readily detected a protein of ~55 kDa in the lysates form $MAN1^{\Delta C}/+$ and $MAN1^{\Delta C}$ flies suggesting that the truncated protein is expressed at similar levels as wildtype MAN1 (Fig. 2C). To determine the subcellular distribution of the truncated MAN1 polypeptide, we analyzed its localization in a variety of tissues, including imaginal discs, salivary glands, gut and muscles of third instar larvae. Immunofluorescence analysis revealed that the $MAN1^{\Delta C}$ protein, like the full-length MAN1, co-localizes with lamin Dm0 at the nuclear rim (Fig. 2E). Thus, the $MAN1^{\Delta C}$ mutants express a MAN1 polypeptide lacking the RRM domain. This deletion does not impact on the general architecture of the nuclear lamina since we did not detect any alterations in the subcellular distribution of Lamin Dm0, Otefin, Bocksbeutel and LBR in $MAN1^{\Delta C}$ mutants (Fig. S3). Similar to *MAN1* null mutants described by Pinto et al., $MAN1^{\Delta C}$ mutants show no detectable effects in nuclear envelope formation. Thus, $MAN1^{\Delta C}$ mutants provide a tractable genetic model for the functional analysis of the C-terminus of MAN1 in BMP signaling.

MAN1 mutants show reduced life span, mobility defects and impaired synaptic transmission

Osteopoikilosis, Buschke–Ollendorf syndrome and melorheostosis, which are caused by heterozygous loss-of-functions in human MAN1, involve the deletion of the C-terminal region of MAN1, which is the interaction domain for R-Smads. Although several phenotypes of *MAN1* and $MAN1^{\Delta C}$ mutants were qualitatively similar and rescued by GAL4 driven expression of a transgenic UAS-*MAN1* construct in either of the mutant strains (Fig. S2B–D and below), we observed a significant increase in lethality in the *MAN1* null mutant when compared to $MAN1^{\Delta C}$ mutants. We focused our analysis on the new $MAN1^{\Delta C}$ to elucidate the specific functions of the Mad-binding RRM-domain of MAN1 in BMP signaling and to exclude unrelated phenotypes caused by potential changes of chromatin localization and gene expression caused by lack of the N-terminal LEM-domain in the null alleles.

MAN1 is required for fly development; about 28% of the expected $MAN1^{\Delta C}$ homozygous adults did not emerge ($n = 662$). The eclosed adults showed a decreased life span (data not shown), male sterility and decreased female fertility when compared to wildtype flies. Interestingly, $MAN1^{\Delta C}$ mutants were also flightless. To determine if mobility in general is affected in $MAN1^{\Delta C}$, we performed a negative geotaxis assay, which reflects coordinated muscle contraction and general motor ability. While more than 90% of the wildtype and $MAN1^{\Delta C}$ heterozygotes reached 10 cm in 20 s, only 30–35% of the $MAN1^{\Delta C}$ homozygotes were able to reach the mark in the same time, suggesting that the motor ability of $MAN1^{\Delta C}$ mutants is impaired (Fig. S6). Similar phenotypes including changes in viability, fertility and locomotion have been described for *MAN1* null mutants by Pinto et al. but it is still not known whether these phenotypes reflect changes in BMP signaling in the fly. The climbing defect of $MAN1^{\Delta C}$ flies could be rescued by transgenic expression of *MAN1* using the UAS/GAL4 system in the mutants. Expression of *MAN1* under the control of the

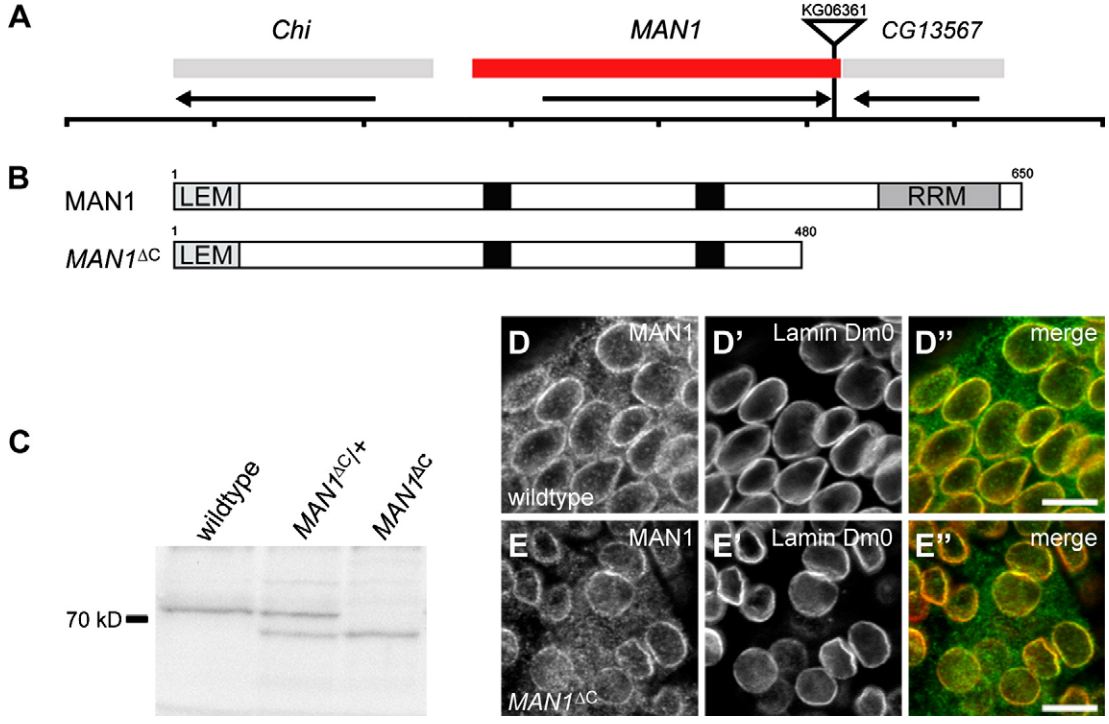

Fig. 2. Generation and characterization of *MAN1* mutant flies. (A) Genomic organization and P-element insertions near the *MAN1* locus. Arrows show direction of transcription. (B) Structural organization of wildtype MAN1 and $MAN1^{\Delta C}$ lacking the RNA recognition motif (RRM). Numbers mark the positions of individual amino acids. Boxes depict transmembrane domains (black), LEM-domain (LEM) and RRM. (C) Western blot analysis reveals the expression of a truncated MAN1 polypeptide in $MAN1^{\Delta C}/+$ and $MAN1^{\Delta C}$ fly lysates compared to the 72 kDa protein expressed in wildtype flies. (D and E) Indirect immunofluorescence microscopy of imaginal discs with MAN1 antibodies shows that $MAN1^{\Delta C}$ is localized at the nuclear rim (E) similar to wildtype MAN1 (D). Specimens were stained with lamin Dm0 specific antibodies to visualize the lamina (D′ and E′). Scale bars: 10 μm.

ubiquitous *actin5C*-GAL4-driver resulted in complete rescue whereas expression of *MAN1* within the presynaptic motoneuron, using the neuronal driver *elav*-GAL4 or within the postsynaptic muscle with the *mef2*-GAL4-driver was not sufficient to fully restore the motor ability (Fig. 3A′). Partial rescue of *MAN1*$^{\Delta C}$ mutants was already observed by just introducing one or two copies of the UAS-MAN1 transgene in the mutants lacking any of the GAL4-drivers (Fig. 3A′). Western blot analysis of MAN1 expression in *MAN1*$^{\Delta C}$ mutants with or without GAL4-drivers revealed high levels of transgenic MAN1 expression even in the absence of GAL4. This leaky expression limited the unambiguous analysis of the potential tissue-specific requirements of MAN1 in muscle or neurons using the climbing assay (Fig. 3A).

To investigate whether the climbing disability of the mutants may be due to defects in muscle development, we first analyzed their morphology. Histological analysis of the major thoracic indirect flight muscles of *MAN1*$^{\Delta C}$ adults did not reveal gross defects in muscle placement or organization (data not shown). Likewise, we detected no obvious phenotypes in muscle size, positioning (Fig. S4A) and fibrillar composition (Fig. S4B and B′) in body wall muscle preparations from *MAN1*$^{\Delta C}$ instar larvae. To ask whether MAN1 is required for muscle innervation we analyzed axon pathfinding in *MAN1*$^{\Delta C}$ mutant embryos using antibodies against Futsch (22C10). We found no defects in embryonic axon guidance. Also in *MAN1*$^{\Delta C}$ mutant larvae all motoneurons had established contact with their appropriate targets

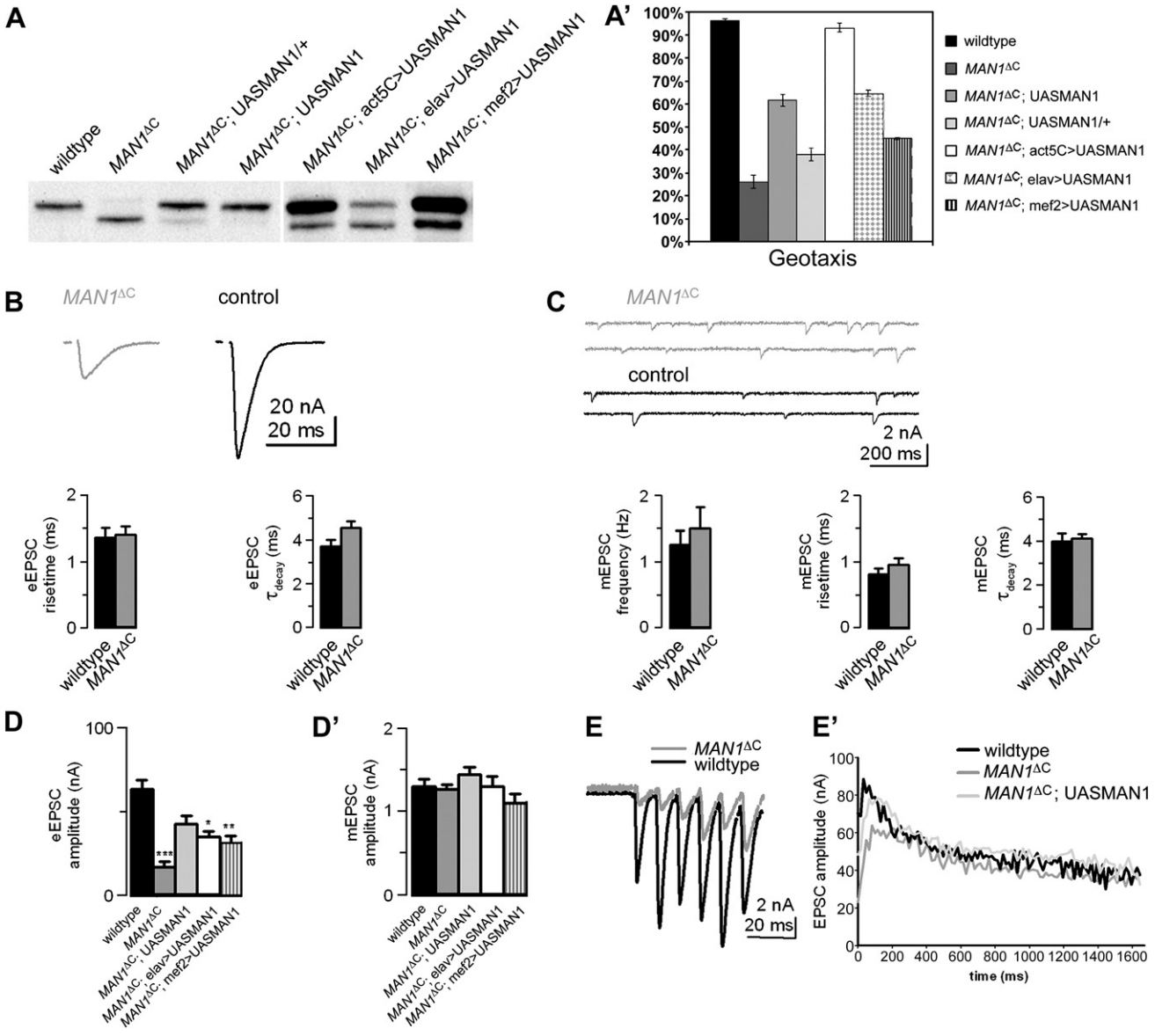

Fig. 3. *MAN1*$^{\Delta C}$ mutants show mobility defects and impaired synaptic transmission. (A) Western blot analysis of MAN1 protein expression in adult fly extracts and (A′) negative geotaxis assay ($p<0.001$) of adult flies of the indicated genotypes: wildtype ($n=40$); *MAN1*$^{\Delta C}$ ($n=40$); flies expressing one (*MAN1*$^{\Delta C}$;UAS*MAN1*/+, $n=42$) or two copies (*MAN1*$^{\Delta C}$;UAS*MAN1*, $n=42$) of UASMAN1 in the *MAN1*$^{\Delta C}$ mutant background and flies expressing UAS*MAN1* under the control of the GAL4-drivers *actin5C*GAL4 (*MAN1*$^{\Delta C}$; act>UAS*MAN1*, $n=36$), *elav*GAL4 (*MAN1*$^{\Delta C}$;elav>UAS*MAN1*, $n=38$), *mef2*GAL4 (*MAN1*$^{\Delta C}$;mef2>UAS*MAN1*, $n=50$) in the *MAN1*$^{\Delta C}$ mutant background. (B) Representative traces of eEPSCs at 0.2 Hz nerve stimulation. The 10–90% risetime and decay time constants of eEPSCs were not significantly altered in *MAN1*$^{\Delta C}$ mutants (grey, $n=7$) compared to controls (black, $n=7$). (C) Sample traces of spontaneous mEPSCs. The 10–90% risetime and decay time constants of mEPSCs as well as the mEPSC frequency were not significantly altered in *MAN1*$^{\Delta C}$ mutants (grey, $n=7$) compared to controls (black, $n=7$). (D and D′) Average eEPSC amplitudes (D) were severely reduced in *MAN1*$^{\Delta C}$ mutant animals (gray, $n=7$), compared to controls (wildtype; black, $n=7$) and could be partially rescued by expression of two copies of UAS*MAN1* without GAL4-driver (*MAN1*$^{\Delta C}$; UAS*MAN1*, light gray, $n=7$) or by expression of one copy of UAS*MAN1* under the control of *elav*GAL4 (*MAN1*$^{\Delta C}$;elav>UAS*MAN1*, white, $n=6$) or *mef2*GAL4 (*MAN1*$^{\Delta C}$; mef2>UAS*MAN1*, striped vertically, $n=5$) while average mEPSC amplitudes (D′) were similar in all genotypes. (E) Representative traces of the first 6 pulses in a 60-Hz train in *MAN1*$^{\Delta C}$ mutant (grey) and control (black). (E′) eEPSC amplitudes during a 60 Hz train (100 pulses) showed transient short-term facilitation, which was much more pronounced in *MAN1*$^{\Delta C}$ mutant (gray, $n=6$) than in control (black, $n=5$), and rescued (*MAN1*$^{\Delta C}$,UAS*MAN1*; light gray, $n=4$) third instar larvae. One asterisk indicates $p<0.05$, two asterisks, $p<0.01$, and three asterisks, $p<0.001$. Error bars indicate SEM.

(Fig. S4C and C′). The synaptic morphology and number of synaptic boutons at the NMJ of *MAN1*$^{\Delta C}$ larvae visualized by Fasciclin II, DiscLarge, Synaptotagmin, Bruchpilot and pMad staining were indistinguishable from the wildtype (Fig. S5). We conclude that the C-terminus of MAN1 is not required for larval muscle development or innervation.

The lack of any evidence for developmental defects at the NMJ of *MAN1*$^{\Delta C}$ suggested that the motor disability of *MAN1*$^{\Delta C}$ mutants might be due to selective defects in synaptic transmission. We measured the electrophysiological properties of muscle 6 in *MAN1*$^{\Delta C}$ mutant larvae. The amplitude of nerve-evoked excitatory postsynaptic currents (eEPSC) in *MAN1*$^{\Delta C}$ was reduced to 27% of wildtype levels (*MAN1*$^{\Delta C}$, -17.0 ± 3.0 nA; control, -63.5 ± 5.2 nA; $n = 7$ each; $p < 0.001$) (Figs. 3B and D). By contrast, the amplitude of spontaneous miniature excitatory postsynaptic currents (mEPSCs) in response to single vesicle fusion events was not altered (Figs. 3C and D′). This indicates that the postsynaptic response to release of a single vesicle, the quantal size, is not the cause of the reduced eEPSC amplitudes. Instead, the impaired synaptic transmission in *MAN1*$^{\Delta C}$ mutants is caused by a decrease in quantal content, the number of vesicles released per action potential. The reduction in quantal content could either be due to a low release probability or to a decrease in the number of readily releasable vesicles. To discriminate between these two possibilities, we analyzed short-term plasticity by applying a high-frequency stimulus train (100 pulses at 60 Hz) to NMJs of *MAN1*$^{\Delta C}$ mutants and controls. During high-frequency stimulation, accumulation of presynaptic calcium increases the highly calcium-dependent vesicle release probability (Katz and Miledi, 1968). The initial facilitation due to the enhancement of release probability was more pronounced in *MAN1*$^{\Delta C}$ mutants than in controls, whereas the onset of the subsequent short-term depression due to vesicle depletion was delayed (Figs. 3E and E′). These alterations in short-term plasticity are consistent with low initial release probability in *MAN1*$^{\Delta C}$ mutants and rule out that the reduced EPSC amplitudes are only caused by a decrease in the number of release-ready vesicles. There were no significant changes in rise time and decay time constants of eEPSCs or mEPSCs (Figs. 3D and E), indicating that the time course of vesicle release and receptor desensitization kinetics were not severely affected.

To address if there is a strong bias in the requirement of MAN1 in muscles or nerves we examined synaptic transmission after re-expression of *MAN1* in the mutants using *mef2*-GAL4 or *elav*-GAL4. Both the pre- or postsynaptic expression of MAN1 could partially rescue the drop in EPSC amplitude detected in *MAN1*$^{\Delta C}$ larvae (Fig. 3D). The expression of two copies of the leaky MAN1 transgene in both tissues even without any driver could also partially rescue all of the described synaptic phenotypes (Figs. 3D and E′). Although the leaky expression of the transgenic protein did not allow us to achieve strict tissue-specific expression using the UAS/GAL4 system, the comparable levels of rescue provided by all GAL4-drivers suggest that MAN1 maybe required both in motoneurons and the muscles.

MAN1 controls wing vein formation

Loss of MAN1 causes LV thickening and an expanded crossvein tissue (Pinto et al., 2008). The molecular mechanisms leading to these phenotypes in *MAN1* deletion mutants are unknown. We analysed our *MAN1*$^{\Delta C}$ mutants to investigate the role of the C-terminal region of MAN1 in BMP signaling during wing development. We found ectopic vein tissue emanating from the PCV in *MAN1*$^{\Delta C}$ adults. The mutants showed no defects in the size of the wing blade or the distance between the LVs (Fig. 4B). The ectopic venation showed incomplete penetrance, with 87% of the mutant female individuals showing additional vein material at one or both wings (Fig. 4G). Ectopic venation was less prominent in the *MAN1*$^{\Delta C}$ males (30–40%), probably due to differences in wing size. This phenotype could be rescued by transgenic expression of MAN1 in the *MAN1*$^{\Delta C}$ mutant background. The *MAN1*$^{\Delta C}$ venation phenotype is indicative of enhanced BMP signaling during wing vein development and resembles loss-of-function mutations in the BMP antagonists *nmo*, *dad* and *kek5* (Evans et al., 2009; Tsuneizumi et al., 1997; Zeng et al., 2007), as well as phenotypes found in flies ectopically expressing Dpp, Gbb or Mad (Haerry et al., 1998; Yu et al., 2000).

If MAN1 antagonizes BMP signaling during CV patterning, increased MAN1 expression would be expected to reduce the activity of the BMP pathway and interfere with CV development. We used MS1096-GAL4 to drive MAN1 expression in the wing. We found defects in the formation of the ACV and the PCV in 90–95% of the emerging adults (Figs. 4C–F and H). The phenotypes ranged from "gaps," where the PCV showed a gap either from L4 or L5 (Fig. 4C), "points," where the PCV was reduced to a point (Fig. 4D), or "PCV absent" (Fig. 4E) and "CV absent" (Fig. 4F) where the PCV or both CVs were missing. In addition, the tip of the longitudinal vein L4 was often compromised leading to truncations (Figs. 4C–F, arrow). These phenotypes are similar to those caused by the *gbb*^{1} and *gbb*^{4} hypomorphic mutations (Ray and Wharton, 2001) and indicate that overexpression of MAN1 reduces Gbb signaling during CV formation.

MAN1 affects Dpp and Gbb signaling during crossvein formation

In frogs and mice, MAN1 acts as a negative regulator of BMP/TGF-β signaling (Osada et al., 2003; Raju et al., 2003; Ishimura et al., 2006; Cohen et al., 2007). To address whether the ectopic venation in *MAN1*$^{\Delta C}$ mutants is a direct result of enhanced BMP signaling, we dissected pupal wings and stained them with an antibody specific to the phosphorylated, active form of Mad (pMad) and DSRF (Montagne et al., 1996). The pMad staining is an indicator of BMP signaling activity in vein regions, whereas DSRF expression delineates intervein territories. In wildtype wings, strong pMad staining is observed in the precursor cells of the LVs around 19–22 h after pupation (AP). From 17–22 h AP, pMAD accumulates in a broad patch of cells in the region of the presumptive PCV. During subsequent stages (24–28 h AP), the pMAD staining becomes refined into a narrow stripe of cells that form the PCV (Shimmi et al., 2005a) (Figs. 5A and B, A″ and B″). We found ectopic pMAD accumulation in an additional patch continuous to the presumptive PCV in *MAN1*$^{\Delta C}$ mutants, indicating that BMP signaling was expanded in this region (Figs. 5C and D, C″ and D″), while expression of DSRF was reduced in the same cells (Figs. 5C′ and D′, C″ and D″). This indicates that more cells in the PCV region activate pMad and acquire the PCV identity. To further characterize the restriction of BMP signaling by MAN1 during CV formation, we monitored the expression of the BMP-responsive gene *cv-2* in pupal wings of *MAN1*$^{\Delta C}$ (Figs. 5G–I). cv-2 is crucial for signaling in the CVs and loss of *cv-2* causes loss of BMP signaling in the developing CVs (Conley et al., 2000; Serpe et al., 2008). In the wildtype, expression of *cv-2* mRNA is first visible broadly around the CVs and the end of the LVs at 21–22 h AP. *cv-2* expression becomes stronger and refines to a narrow stripe at 28–29 h AP (Figs. 5G and G′). In *MAN1*$^{\Delta C}$ mutants, the initiation of cv-2 expression was indistinguishable from the wildtype. However, *cv-2* expression remained detectable at the region of ectopic vein formation 29 h AP (Figs. 5H and H′). This indicates that the C-terminus of MAN1 is required to restrict *cv-2* expression and define the number of cells that will respond to enhanced BMP signaling and form the CV.

The similarity of the CV phenotypes caused by MAN1 overexpression during wing development with the defects of hypomorphic mutations reducing BMP signaling prompted us to test whether MAN1 overexpression directly interferes pMad activation. MAN1 overexpression abolished pMad accumulation at the presumptive PCV and reduced it in the regions of the presumptive LVs (Figs. 5E and F, E″ and F″). This indicates that ectopic expression of MAN1 is sufficient to

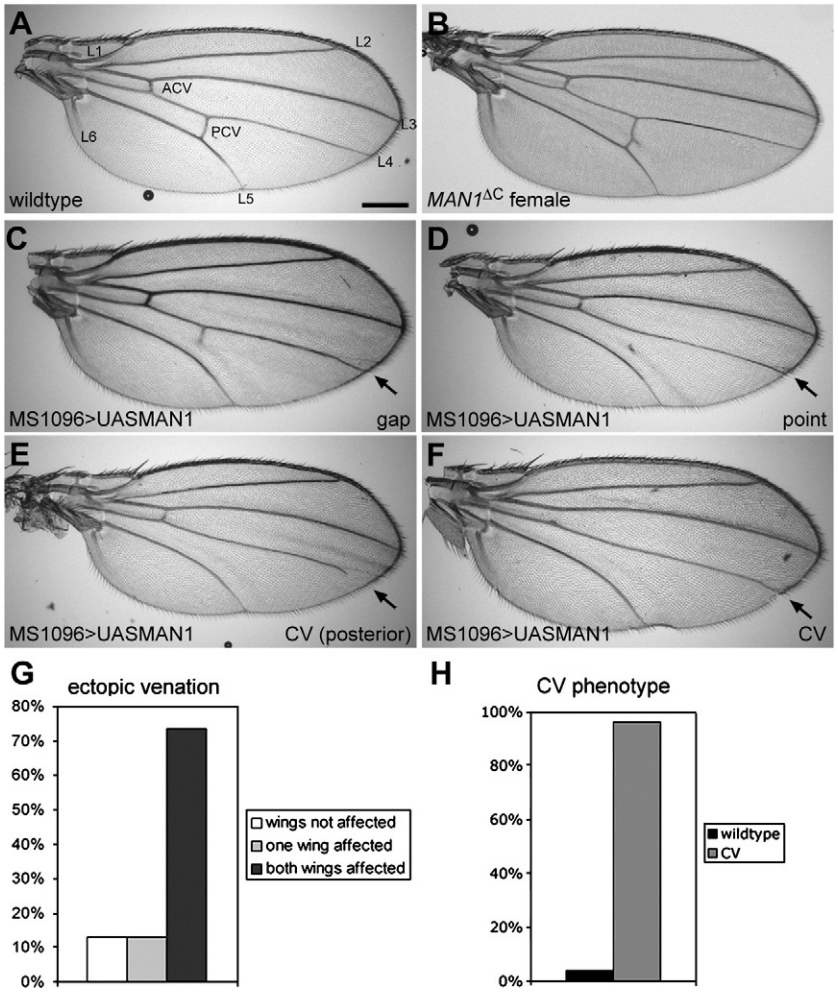

Fig. 4. Modulation of MAN1 expression affects wing vein development. (A) Wildtype adult wing, showing the location of the longitudinal veins (L1-L6), the anterior (ACV) and posterior crossvein (PCV). (B) Wings from *MAN1*$^{\Delta C}$ adults show ectopic veins emanating from the PCV. (C–F) Wing patterning defects caused by *MS1096*GAL4>UAS*MAN1* overexpression. The phenotypes affect the ACV, PCV and the distal tip of L4 (arrow). In these flies, the phenotypes were described as "gap" (C), either from L5 as an posterior gap or L4 as an anterior gap (not shown); "point" (D); "CV posterior" leaving the ACV unaffected (E); or "CV" where both the ACV and the PCV are missing (F). (G) Quantification of the ectopic venation in *MAN1*$^{\Delta C}$ females ($n=76$, $p<0.001$, chi-square). (H) Quantification of crossveinless (CV) phenotype observed by overexpression of UAS*MAN1* using *MS1096*GAL4 ($n=237$, $p<0.001$, chi-square).

reduce the levels of BMP signaling during PCV formation. Consistently, DSRF expression was expanded (Figs. 5E′ and F′) and the expression *cv-2* was lost in the presumptive PCV region (Figs. 5I and I′).

Gbb signaling induces MAN1 expression in the pupal wing

BMP signaling plays several key roles during wing vein development: First, during the initial specification of vein and intervein regions in the third instar imaginal wing disc. Later it also maintains and refines the LVs and finally it specifies CVs during pupal wing development. The analysis of MAN1 expression during larval and pupal development revealed that MAN1 *RNA* was uniform in the larval imaginal discs, while a clear staining pattern can be seen during pupal wing development that corresponds to the presumptive LVs (Fig. 6A). The higher levels of MAN1 RNA in the cells with increased BMP signaling activity suggested that MAN1 expression might be positively regulated by BMP activity during pupal development. To address whether *MAN1* expression can respond to Gbb signaling, we examined its expression in pupal wings expressing a UAS-*gbb* transgene in the posterior compartment under the control of the *en*-GAL4-driver. Ectopic expression of Gbb in the posterior compartment resulted in ectopic upregulation of *MAN1* transcripts in the entire posterior region (Figs. 6B, B′, and C). This indicates that MAN1 is also a transcriptional target of the BMP signaling pathway in the pupal wing.

To address if Gbb signaling can also induce MAN1 expression in the larval imaginal wing discs we analysed MAN1 expression in larval wing discs and pupal wing of *en*GAL4>UAS-*gbb* animals in parallel. Antibody stainings for pMad showed that ectopic Gbb expression resulted in enhanced BMP signaling predominantly in the posterior compartments of both larval wing discs (Figs. 6E′, E″, and F) and pupal wings (Figs. 6D, D″, and G). As expected from the RNA analysis, ectopic expression of Gbb in the pupal wing resulted in significantly increased MAN1 protein levels predominantly in the posterior compartment (Figs. 6D′, D″, and G). However, we did not detect any increase in MAN1 levels in the posterior compartment of larval imaginal wing disc (Figs. 6E′, E″, and F). These results suggest that BMP signaling mediated by Gbb upregulates MAN1 expression during vein formation in pupal wings. The suggested inhibitory feedback loop may limit the duration or levels of BMP signaling during crossvein formation.

MAN1 antagonizes dpp and gbb signaling in the wing and at the neuromuscular junction

Since MAN1 modulates BMP signaling during CV formation, we tested whether the ectopic venation phenotype of *MAN1*$^{\Delta C}$ mutants can be suppressed by a decrease of the *Drosophila* BMPs, Dpp and Gbb. Eighty-seven percent of *MAN1*$^{\Delta C}$ mutant females show extra vein material. Strikingly, only 14% of the *MAN1*$^{\Delta C}$ flies heterozygous for

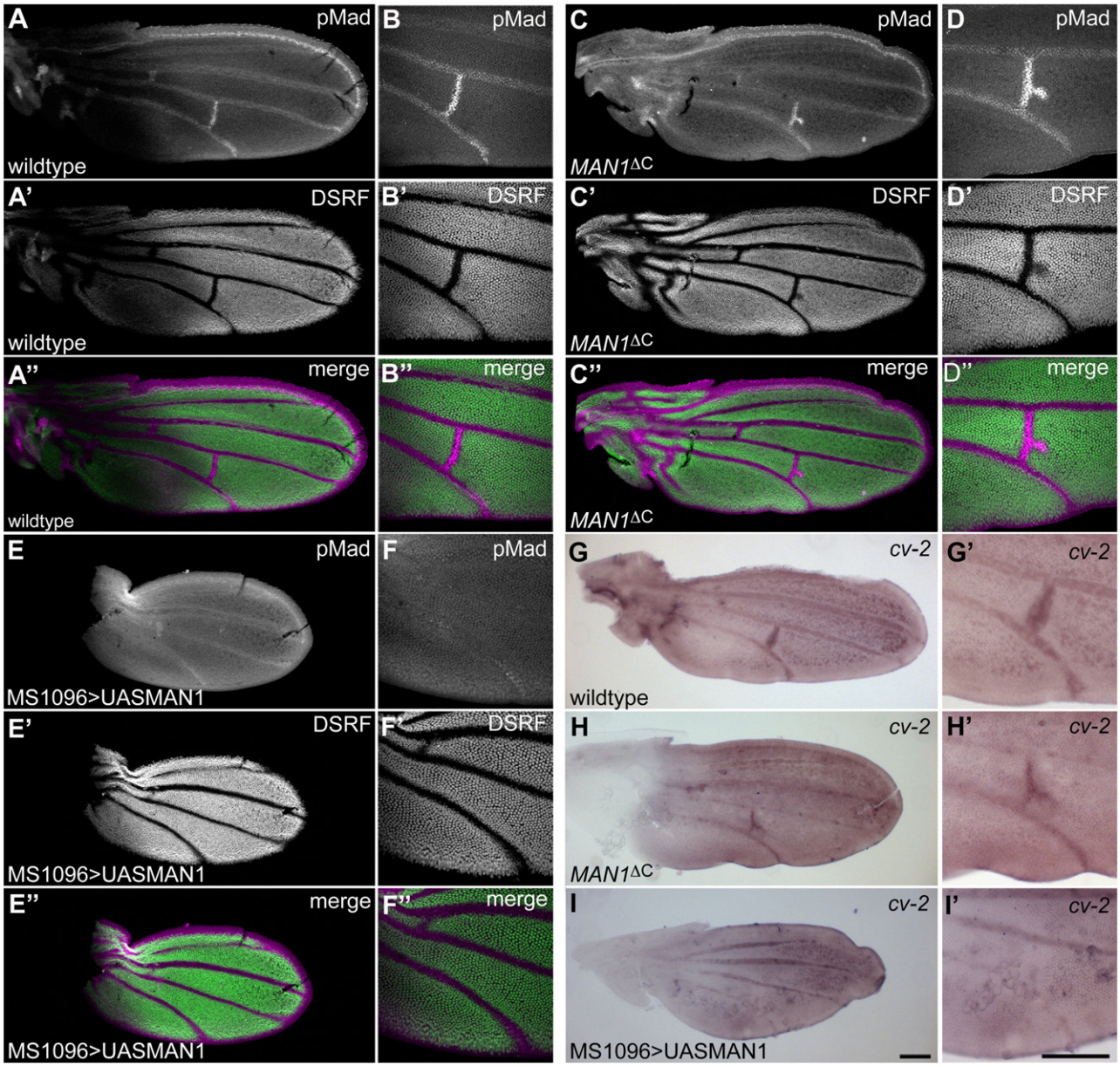

Fig. 5. MAN1 affects Dpp and Gbb signaling during crossvein formation. (A and B) Anti-pMad (A and B, magenta in A″ and B″) and anti-DSRF (A′ and B′, green in A″ and B″) staining in wild-type pupal wings 28 h after pupation. (A″) Note that the intervein marker DSRF does not co-localize with pMad, which accumulates in the LVs and the CVs. (B–B″) Magnification of the PCV shown in (A) to (A″). (C and D) Anti-pMad (C and D, magenta in C″ and D″) and anti-DSRF (C′ and D′, green in C″ and D″) staining in *MAN1*$^{\Delta C}$ pupal wings 28 h after pupation. Note that the pMad signaling is expanded at the region of the presumptive ectopic vein emanating from the PCV (C″). (D–D″) Magnification of the PCV shown in (C) to (C″). (E and F) Anti-pMad (E and F, magenta in E″ and F″) and anti-DSRF (E′ and F′, green in E″ and F″) staining in pupal wings where UAS*MAN1* is ectopically expressed under the control of *MS1096*GAL4. Note that the pMad staining is completely absent while the DSRF staining is expanded in the region of the presumptive crossvein. Magnification of the presumptive crossvein region in (E) to (E″). In situ hybridization with *crossveinless-2* (*cv-2*) probe in the pupal wings of wildtype (G and G′), *MAN1*$^{\Delta C}$ mutants (B and B′) and wings where UASMAN1 is ectopically expressed under the control of *MS1096*GAL4 (I and I′). Note the presence of *cv-2* in the ectopic vein in *MAN1*$^{\Delta C}$ mutants and its complete absence when UAS*MAN1* is overexpressed in the wing. Scale bars: 20 μm.

dpp^{S11} mutations and 15% of *MAN1*$^{\Delta C}$ mutants heterozygous for *gbb*^{1} showed extra venation (Fig. 7A). Thus, reduction of the Dpp or Gbb level suppresses the wing vein defects of *MAN1*$^{\Delta C}$ mutants. This suggests that MAN1 normally acts to limit BMP signaling during vein patterning. Does reduction of BMP signaling also ameliorate the synaptic defects of *MAN1*$^{\Delta C}$? Gbb is so far the only known BMP ligand at the NMJ. We monitored the eEPSC amplitudes in muscle 6 of *MAN1*$^{\Delta C}$ mutants, in *gbb*^{1}/+ heterozygotes, and *MAN1*$^{\Delta C}$*gbb*^{1}/*MAN1*$^{\Delta C}$ + larvae. The *MAN1*$^{\Delta C}$ mutants showed a strong reduction of eEPSC amplitude compared to the *gbb*^{1}heterozygotes and the wildtype control. However, the low eEPSC amplitude of *MAN1*$^{\Delta C}$ mutants was increased drastically in the mutants carrying a single copy of the *gbb*^{1} allele (Fig. 7B). Therefore, reduction of Gbb levels does not only suppress the wing venation phenotype, but it also strongly ameliorates the synaptic transmission defects of *MAN1*$^{\Delta C}$ mutants. The dosage sensitive genetic interactions indicate that MAN1 limits BMP signaling both during wing venation and synaptic transmission at the NMJ.

Discussion

MAN1, a cell-specific inhibitor of BMP signaling in crossveins

Restriction and refinement of BMP signaling is achieved by the regulation of ligand transport and availability or by control of pMad activity. Crossvein development in the pupal wing has provided an

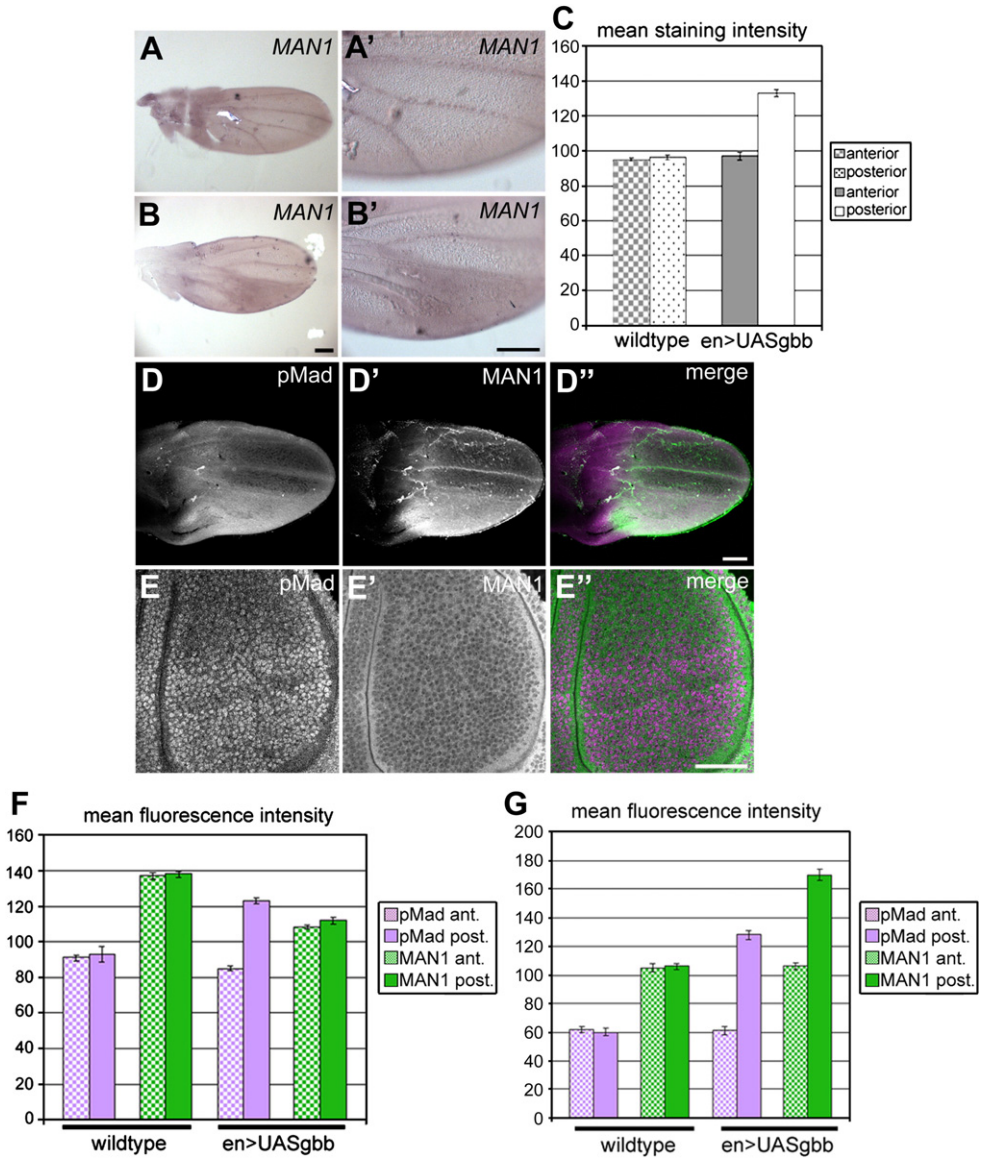

Fig. 6. Gbb signaling induces MAN1 expression in the pupal wing but not in the third instar imaginal wing disc. Posterior expression of UAS*Gbb* under the control of *engrailed*GAL4 (*en*>UAS*Gbb*) result in ectopic expression of MAN1 during pupal wing development. (A–C) In situ hybridization with *MAN1* probe in the anterior and posterior half of pupal wings in wildtype (A) and en>UAS*Gbb* (B) pupal wings 28 h after pupation. (C) Quantification of mean staining intensity in the anterior and posterior half of pupal wings in wildtype and *en*>UAS*Gbb* pupal wings. Enhanced Gbb signaling in the posterior part of the pupal wing blade (D′ and D″) or the wing imaginal disc (E and E″) is monitored by staining for pMad. (F) Quantification of MAN1 (green) and pMad (magenta) antibody staining in the anterior and posterior half of imaginal wing discs in wildtype and en>UAS*Gbb* third instar larvae. Note that expression of pMad, but not expression of MAN1 is enhanced in the posterior part of the imaginal disc ($p<0.001$). (G) Quantification of MAN1 (green) and pMad (magenta) antibody staining in the anterior and posterior half of pupal wings in wildtype and en>UAS*Gbb* pupal wings 28 h after pupation. Note that expression of pMad and MAN1 is enhanced in the posterior part of the pupal wing blade ($p<0.001$). Error bars indicate SEM. Scale bars: 20 μm; 50 μm.

attractive system to study BMP signaling in *Drosophila* due to its high sensitivity to manipulations in BMP signaling levels (Christoforou et al., 2008; Conley et al., 2000; Denholm et al., 2005; Evans et al., 2009; Ralston and Blair, 2005; Serpe et al., 2005; Shimmi et al., 2005a; Vilmos et al., 2005; Zeng et al., 2007). We have identified a new antagonistic role for the LEM-domain protein MAN1 in BMP signaling during CV formation. Our genetic analysis indicates that MAN1 is required for the spatial refinement of a small subset of BMP signaling events. *MAN1*$^{\Delta C}$ mutants display expanded pMad accumulation and maintain expression of the BMP-responsive gene *cv-2* in cells abutting the CVs. Reduction in the level of BMP ligands in *MAN1*$^{\Delta C}$ mutants ameliorates the ectopic venation phenotype. How does MAN1 affect CV patterning? Like wildtype flies, *MAN1*$^{\Delta C}$ mutants activate Mad and cv-2 expression in a broad cellular domain at the initiation of CV formation (~20 h AP) (Serpe et al., 2008; data not shown). In the wildtype, this domain becomes refined to a distinct row of cells during the next 10 h of development. The retained expanded accumulation of nuclear pMad and cv-2 expression in more cells in *MAN1*$^{\Delta C}$ mutants suggests that MAN1 refines the BMP response by defining the number of cells that continue to respond to BMP.

INM proteins and nuclear lamina components are ubiquitous proteins, generally expressed at uniform levels in all cells (Gruenbaum et al., 2005). How can a ubiquitous INM protein, like MAN1, participate in localized BMP signaling? We found that *MAN1* mRNA levels can be modulated by Gbb signaling. To our knowledge this is the first example of dynamic regulation of an INM protein-coding gene by signaling. The selective upregulation of MAN1 in pupal wings suggests that the BMP response in the presumptive CV cells depends on a delicate balance between the activation of pMad by Gbb/Dpp signals and the antagonistic function of MAN1 on pMad in the nucleus. A negative feedback loop caused by increased levels of MAN1 in the

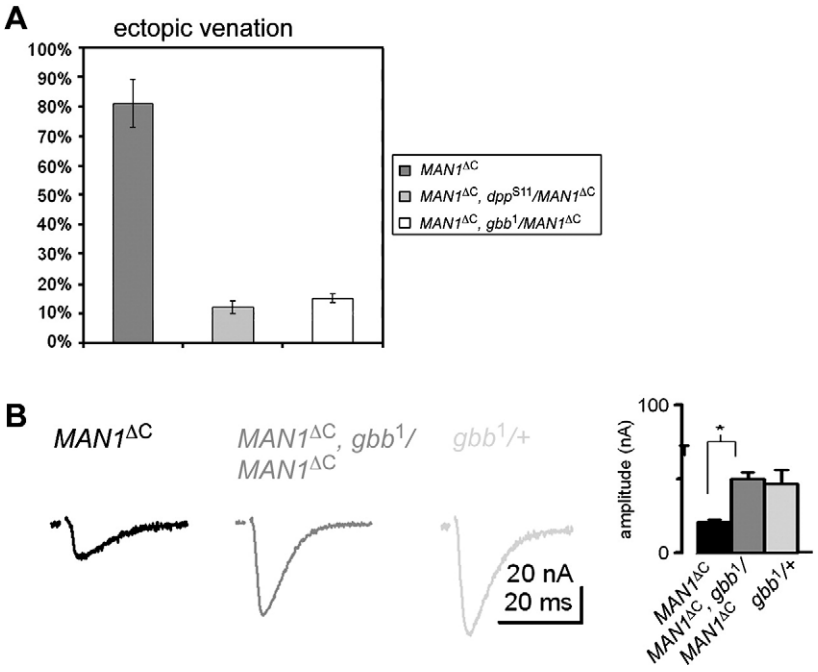

Fig. 7. *MAN1* antagonizes *dpp* and *gbb* signaling in wings and at the neuromuscular junction. (A) Heterozygosity for the gbb^1 ($n=144$) or dpp^{S11} ($n=165$) mutant suppresses the ectopic venation of $MAN1^{\Delta C}$ mutants ($n=106$), Student's t test ($p<0.001$). (B) Representative traces of eEPSCs at 0.2 Hz nerve stimulation and average eEPSC amplitudes recorded from $MAN1^{\Delta C}$ ($n=5$), heterozygous gbb^1 ($n=5$) and $MAN1^{\Delta C}$,$gbb^1/MAN1^{\Delta C}$ ($n=10$) mutant larvae demonstrating that gbb suppresses the $MAN1^{\Delta C}$ defect in evoked release. Student's t test ($p<0.05$).

responding cells may set a threshold for the BMP response and select the number of cells that form the CV.

Previous yeast two-hybrid studies suggested that *Drosophila* MAN1 binds to Mad with its C-terminal domain but did not proof the Mad binding with an independent method (Pinto et al., 2008). In contrast, we have performed a detailed binding study using GST-constructs and co-immunoprecipitations to address this question. We show that MAN1 binds directly to Mad through its conserved C-terminal RRM domain. In addition to the RRM domain, we were able to identify a novel, second binding site in the N-terminal region of MAN1, which does not overlap with the BAF-binding LEM-domain. The analysis of the *MAN1* null mutant suggests that this second binding site contributes to the function of MAN1 *in vivo*. The frequency and extend of ectopic venation seen in *MAN1* mutants is increased compared to the $MAN1^{\Delta C}$ mutants. This suggests that both binding sites may contribute to the restriction and refinement of BMP signaling during pupal wing development. Furthermore, *MAN1* deletion mutants showed an even stronger synaptic phenotype than seen in $MAN1^{\Delta C}$ mutants, with a reduction of the amplitude of eEPSCs to 14% of wildtype levels. On the other hand the N-terminal domain of MAN1 interacts with chromatin factors and overexpression of a mammalian homolog can interfere with INM integrity (Brachner et al., 2005). Further biochemical and genetic analysis of the N-terminal domain is required to dissect apart its potential roles in nuclear envelope formation and signaling.

MAN1 in presynaptic signaling at the neuromuscular junction

Mutations in lamins and lamin-binding proteins are associated with a wide spectrum of human diseases, commonly referred to as laminopathies. Despite the range of mutant studies in worms, frogs and mice, MAN1 has not previously been implicated in synaptic signaling. Although muscle innervation and NMJ morphology are normal, we found that synaptic transmission is severely impaired and short-term synaptic plasticity is altered in $MAN1^{\Delta C}$ mutants. The predominant localization of MAN1 at the INM suggests a role in regulating genes required for synapse function. Interestingly, the innervation pattern and NMJ morphology are altered in two mouse mutants of the *LMNA* gene, coding for lamins A and C (Méjat et al., 2009). In contrast to our $MAN1^{\Delta C}$ mutant, *LMNA* mutants showed drastically altered nuclear structure and mispositioning of nuclei in muscle fibers and neuronal cells.

Synaptic growth, morphology and function are regulated by BMP signaling. Reduction of Gbb levels in $MAN1^{\Delta C}$ mutants ameliorates synaptic transmission defects, indicating that the synaptic phenotype in *MAN1* mutants reflects changes in BMP signaling at the NMJ. However, $MAN1^{\Delta C}$ mutants do not show enhanced neurotransmitter release, and synaptic overgrowth like mutants in *dad*, another BMP inhibitor at the NMJ (Sweeney and Davis, 2002; Dudu et al., 2006; O'Connor-Giles et al., 2008). These phenotypic differences and the enhanced expressivity of presynaptic defects in $MAN1^{\Delta C}$ mutants suggest that the truncated protein may be sufficient to support BMP signaling during synaptic growth. Alternatively MAN1 maybe selectively required for synaptic transmission. Like MAN1, *gbb* is expressed pre- and postsynaptically and pMad has been shown to be necessary both in the neuron and in the muscle (McCabe et al., 2003). Postsynaptic BMP signaling also occurs at the larval NMJ. pMad is localized postsynaptically and additional Mad phosphorylation occurs in regions facing the presynaptic active zone of neurotransmitter release (Dudu et al., 2006). Thus, it is possible that MAN1 affects retro- and anterograde BMP signaling by monitoring pMad activity both in neurons and muscle. The distinct BMP functions at the NMJ are likely to be subjected to negative regulation to fine tune pMad activity. Such regulation can occur at various levels, including endocytic regulation of BMP receptor trafficking, as shown for *nervous wreck* (*nwk*) or regulation via inhibitory Smads, as shown for *dad*. It will be interesting to see if the antagonistic function of MAN1 is specific to distinct BMP signaling events at the NMJ.

How does MAN1 antagonize BMP signaling?

BMP signaling has been shown to be regulated at multiple levels, including R-Smad dephosphorylation and its translocation into the

cytoplasm. The vertebrate R-Smads are known to shuttle between cytoplasm and the nucleus. Upon ligand binding and receptor activation, R-Smads are phosphorylated, form a ternary complex with the Co-Smad and the complex is then translocated and retained in the nucleus (O'Connor et al., 2006). One way of regulation is the dephosphorylation of R-Smads in the nucleus, where they are proposed to detach from the Co-Smad, resulting in a rapid transfer back to the cytoplasm (Chen et al., 2006). What about MAN1? Overexpression of MAN1 reduces the levels of pMad and cv-2 expression leading to CV loss. As an INM protein, MAN is unlikely to interfere with Mad phosphorylation in the cytoplasm. MAN1 is more likely to control the distribution and stability of pMad in the nucleus. Consistent with this idea, overexpression of MAN1 affects a certain level of free pMad in the nucleus, demonstrated by its localization at the nuclear periphery (Fig. S7). Phospho-Mad function may be suppressed through its redistribution, thereby preventing its access to downstream target genes. It is important to note however, that these results do not exclude a more complex model, which involves interactions of MAN1 and pMad with other regulators or membrane associated components. A Mad phosphatase has been recently described in *Drosophila* (Chen et al., 2006). It will be interesting to assess its potential binding to MAN1 and its localization in *MAN1* mutants to further elucidate the molecular function of MAN1 in BMP signaling.

Acknowledgments

We thank D. Andrew, E. Buchner, E. Chen, C.-H. Heldin, and S. Thor for reagents and strains. We are grateful to our colleagues for comments on the manuscript. The work was supported by grants from Cancerfonden and the Swedish research Council to C.S. N.W. was supported by a DFG postdoctoral scholarship.

Appendix A. Supplementary data

Supplementary data associated with this article can be found, in the online version, at doi:10.1016/j.ydbio.2009.11.036.

References

Aberle, H., Haghighi, A.P., Fetter, R.D., McCabe, B.D., Magalhães, T.R., Goodman, C.S., 2002. Wishful thinking encodes a BMP type II receptor that regulates synaptic growth in *Drosophila*. Neuron 33, 545–558.

Affolter, M., Basler, K., 2007. The Decapentaplegic morphogen gradient: from pattern formation to growth regulation. Nat. Rev. Genet. 8, 663–674.

Arora, K., Levine, M.S., O'Connor, M.B., 1994. The screw gene encodes a ubiquitously expressed member of the TGF-beta family required for specification of dorsal cell fates in the *Drosophila* embryo. Genes Dev. 8, 2588–2601.

Bengtsson, L., 2007. What MAN1 does to the Smads. TGFbeta/BMP signaling and the nuclear envelope. FEBS J. 274, 1374–1382.

Blair, S.S., 2007. Wing vein patterning in *Drosophila* and the analysis of intercellular signaling. Annu. Rev. Cell. Dev. Biol. 23, 293–319.

Brachner, A., Reipert, S., Foisner, R., Gotzmann, J., 2005. LEM2 is a novel MAN1-related inner nuclear membrane protein associated with A-type lamins. J. Cell. Sci. 118, 5797–5810.

Chen, H.B., Shen, J., Ip, Y.T., Xu, L., 2006. Identification of phosphatases for Smad in the BMP/DPP pathway. Genes Dev. 20, 648–653.

Christoforou, C.P., Greer, C.E., Challoner, B.R., Charizanos, D., Ray, R.P., 2008. The detached locus encodes *Drosophila* Dystrophin, which acts with other components of the Dystrophin Associated Protein Complex to influence intercellular signaling in developing wing veins. Dev. Biol. 313, 519–532.

Cohen, T.V., Kosti, O., Stewart, C.L., 2007. The nuclear envelope protein MAN1 regulates TGFbeta signaling and vasculogenesis in the embryonic yolk sac. Development 134, 1385–1395.

Collins, C.A., DiAntonio, A., 2007. Synaptic development: insights from *Drosophila*. Curr. Opin. Neurobiol. 17, 35–42.

Conley, C.A., Silburn, R., Singer, M.A., Ralston, A., Rohwer-Nutter, D., Olson, D.J., Gelbart, W., Blair, S.S., 2000. Crossveinless 2 contains cysteine-rich domains and is required for high levels of BMP-like activity during the formation of the cross veins in *Drosophila*. Development 127, 3947–3959.

Denholm, B., Brown, S., Ray, R.P., Ruiz-Gomez, M., Skaer, H., Hombria, J.C., 2005. crossveinless-c is a RhoGAP required for actin reorganisation during morphogenesis. Development 132, 2389–2400.

Dudu, V., Bittig, T., Entchev, E., Kicheva, A., Jülicher, F., González-Gaitán, M., 2006. Postsynaptic mad signaling at the *Drosophila* neuromuscular junction. Curr. Biol. 16, 625–635.

Eaton, B.A., Davis, G.W., 2005. LIM Kinase1 controls synaptic stability downstream of the type II BMP receptor. Neuron 47, 695–708.

Evans, T.A., Haridas, H., Duffy, J.B., 2009. Kekkon5 is an extracellular regulator of BMP signaling. Dev. Biol. 326, 36–46.

Gruenbaum, Y., Margalit, A., Goldman, R.D., Shumaker, D.K., Wilson, K.L., 2005. The nuclear lamina comes of age. Nat. Rev. Mol. Cell. Biol. 6, 21–31.

Haerry, T.E., Khalsa, O., O'Connor, M.B., Wharton, K.A., 1998. Synergistic signaling by two BMP ligands through the SAX and TKV receptors controls wing growth and patterning in *Drosophila*. Development 125, 3977–3987.

Haghighi, A.P., McCabe, B.D., Fetter, R.D., Palmer, J.E., Hom, S., Goodman, C.S., 2003. Retrograde control of synaptic transmission by postsynaptic CaMKII at the *Drosophila* neuromuscular junction. Neuron 39, 255–267.

Hellemans, J., Preobrazhenska, O., Willaert, A., Debeer, P., Verdonk, P.C., Costa, T., Janssens, K., Menten, B., Van Roy, N., Vermeulen, S.J., et al., 2004. Loss-of-function mutations in LEMD3 result in osteopoikilosis, Buschke–Ollendorff syndrome and melorheostosis. Nat. Genet. 36, 1213–1218.

Hellemans, J., Debeer, P., Wright, M., Janecke, A., Kjaer, K.W., Verdonk, P.C., Savarirayan, R., Basel, L., Moss, C., Roth, J., et al., 2006. Germline LEMD3 mutations are rare in sporadic patients with isolated melorheostosis. Hum. Mutat. 27, 290.

Ishimura, A., Ng, J.K., Taira, M., Young, S.G., Osada, S.I., 2006. Man1, an inner nuclear membrane protein, regulates vascular remodeling by modulating transforming growth factor {beta} signaling. Development 133, 3919–3928.

Ishimura, A., Chida, S., Osada, S., 2008. Man1, an inner nuclear membrane protein, regulates left-right axis formation by controlling nodal signaling in a node-independent manner. Dev. Dyn. 237, 3565–3576.

Jiang, X., Xia, L., Chen, D., Yang, Y., Huang, H., Yang, L., Zhao, Q., Shen, L., Wang, J., Chen, D., 2008. Otefin, a nuclear membrane protein, determines the fate of germline stem cells in *Drosophila* via interaction with Smad complexes. Dev. Cell. 14, 494–506.

Katz, B., Miledi, R., 1968. The role of calcium in neuromuscular facilitation. J. Physiol. 195, 481–492.

Kawamura, A., Ochiai, T., Tan-Kinoshita, M., Suzuki, H., 2005. Buschke–Ollendorff syndrome: three generations in a Japanese family. Pediatr. Dermatol. 22, 133–137.

Khalsa, O., Yoon, J., Torres-Schumann, S., Wharton, K.A., 1998. TGF-b/BMP superfamily members, gbb-60A and dpp, cooperate to provide pattern information and establish cell identity in the *Drosophila* wing. Development 125, 2723–2734.

Lang, C., Krohne, G., 2003. Lamina-associated polypeptide 2beta (LAP2beta) is contained in a protein complex together with A- and B-type lamins. Eur. J. Cell. Biol. 82, 143–153.

Lin, F., Morrison, J.M., Wu, W., Worman, H.J., 2005. MAN1, an integral protein of the inner nuclear membrane, binds Smad2 and Smad3 and antagonizes transforming growth factor-beta signaling. Hum. Mol. Genet. 14, 437–445.

Liu, J., Lee, K.K., Segura-Totten, M., Neufeld, E., Wilson, K.L., Gruenbaum, Y., 2003. MAN1 and emerin have overlapping function(s) essential for chromosome segregation and cell division in *Caenorhabditis elegans*. Proc. Natl. Acad. Sci. U. S. A. 100, 4598–4603.

Marques, G., Musacchio, M., Shimell, M.J., Wunnenberg-Stapleton, K., Cho, K.W., O'Connor, M.B., 1997. Production of a DPP activity gradient in the early *Drosophila* embryo through the opposing actions of the SOG and TLD proteins. Cell 91, 417–426.

Marques, G., Bao, H., Haerry, T.E., Shimell, M.J., Duchek, P., Zhang, B., O'Connor, M.B., 2002. The *Drosophila* BMP type II receptor Wishful Thinking regulates neuromuscular synapse morphology and function. Neuron 33, 529–543.

McCabe, B.D., Marques, G., Haghighi, A.P., Fetter, R.D., Crotty, M.L., Haerry, T.E., Goodman, C.S., O'Connor, M.B., 2003. The BMP homolog Gbb provides a retrograde signal that regulates synaptic growth at the *Drosophila* neuromuscular junction. Neuron 39, 241–254.

McCabe, B.D., Hom, S., Aberle, H., Fetter, R.D., Marques, G., Haerry, T.E., Wan, H., O'Connor, M.B., Goodman, C.S., Haghighi, A.P., 2004. Highwire regulates presynaptic BMP signaling essential for synaptic growth. Neuron 41, 891–905.

Méjat, A., Decostre, V., Li, J., Renou, L., Kesari, A., Hantaï, D., Stewart, C.L., Xiao, X., Hoffman, E., Bonne, G., Misteli, T., 2009. Lamin A/C-mediated neuromuscular junction defects in Emery–Dreifuss muscular dystrophy. J. Cell. Biol. 184, 31–44.

Montagne, J., Groppe, J., Guillemin, K., Krasnow, M.A., Gehring, W.J., Affolter, M., 1996. The *Drosophila* Serum Response Factor gene is required for the formation of intervein tissue of the wing and is allelic to blistered. Development 122, 2589–2597.

O'Connor, M., Umulis, B.D., Othmer, H.G., Blair, S.S., 2006. Shaping BMP morphogen gradients in the *Drosophila* embryo and pupal wing. Development 133, 183–193.

O'Connor-Giles, K.M., Ho, L.L., Ganetzky, B., 2008. Nervous wreck interacts with thickveins and the endocytic machinery to attenuate retrograde BMP signaling during synaptic growth. Neuron 58, 507–518.

Osada, S., Ohmori, S.Y., Taira, M., 2003. XMAN1, an inner nuclear membrane protein, antagonizes BMP signaling by interacting with Smad1 in *Xenopus* embryos. Development 130, 1783–1794.

Pan, D., Estevez-Salmeron, L.D., Stroschein, S.L., Zhu, X., He, J., Zhou, S., Luo, K., 2005. The integral inner nuclear membrane protein MAN1 physically interacts with the R-Smad proteins to repress signaling by the transforming growth factor-{beta} superfamily of cytokines. J. Biol. Chem. 280, 15992–16001.

Pinto, B.S., Wilmington, S.R., Hornick, E.E., Wallrath, L.L., Geyer, P.K., 2008. Tissue-specific defects are caused by loss of the *Drosophila* MAN1 LEM domain protein. Genetics 180, 133–145.

Raftery, L.A., Sutherland, D.J., 1999. TGF-beta family signal transduction in *Drosophila* development: from Mad to Smads. Dev. Biol. 210, 251–268.

Raju, G.P., Dimova, N., Klein, P.S., Huang, H.C., 2003. SANE, a novel LEM domain protein, regulates bone morphogenetic protein signaling through interaction with Smad1. J. Biol. Chem. 278, 428–437.

Ralston, A., Blair, S.S., 2005. Long-range Dpp signaling is regulated to restrict BMP signaling to a crossvein competent zone. Dev. Biol. 280, 187–200.

Rawson, J.M., Lee, M., Kennedy, E.L., Selleck, S.B., 2003. *Drosophila* neuromuscular synapse assembly and function require the TGF-b type I receptor saxophone and the transcription factor Mad. J. Neurobiol. 55, 134–150.

Ray, R.P., Wharton, K.A., 2001. Context-dependent relationships between the BMPs gbb and dpp during development of the *Drosophila* wing imaginal disk. Development 128, 3913–3925.

Serpe, M., Umulis, D., Ralston, A., Chen, J., Olson, D.J., Avanesov, A., Othmer, H., O'Connor, M.B., Blair, S.S., 2008. The BMP-binding protein Crossveinless 2 is a short-range, concentration-dependent, biphasic modulator of BMP signaling in *Drosophila*. Dev Cell. 14, 940–953.

Sekelsky, J.J., Newfeld, S.J., Raftery, L.A., Chartoff, E.H., Gelbart, W.M., 1995. Genetic characterization and cloning of mothers against dpp, a gene required for decapentaplegic function in *Drosophila melanogaster*. Genetics 139, 1347–1358.

Serpe, M., Ralston, A., Blair, S.S., O'Connor, M.B., 2005. Matching catalytic activity to developmental function: Tolloid-related processes Sog in order to help specify the posterior crossvein in the *Drosophila* wing. Development 132, 2645–2656.

Shimmi, O., Ralston, A., Blair, S.S., O'Connor, M.B., 2005a. The crossveinless gene encodes a new member of the Twisted gastrulation family of BMP-binding proteins which, with Short gastrulation, promotes BMP signaling in the crossveins of the *Drosophila* wing. Dev. Biol 282, 70–83.

Shimmi, O., Umulis, D., Othmer, H., O'Connor, M.B., 2005b. Facilitated transport of a Dpp/Scw heterodimer by Sog/Tsg leads to robust patterning of the *Drosophila* blastoderm embryo. Cell 120, 873–886.

Sweeney, S.T., Davis, G.W., 2002. Unrestricted synaptic growth in spinster-a late endosomal protein implicated in TGF-beta-mediated synaptic growth regulation. Neuron 36, 403–416.

Tsuneizumi, K., Nakayama, T., Kamoshida, Y., Kornberg, T.B., Christian, J.L., Tabata, T., 1997. Daughters against dpp modulates dpp organizing activity in *Drosophila* wing development. Nature 389, 627–631.

Vilmos, P., Sousa-Neves, R., Lukacsovich, T., Marsh, J.L., 2005. Crossveinless defines a new family of Twisted-gastrulation-like modulators of bone morphogenetic protein signaling. EMBO Rep. 6, 262–267.

Wagner, N., Krohne, G., 2007. LEM-domain proteins: new insights into lamin-interacting proteins. Int. Rev. Cytol. 261, 1–46.

Wagner, N., Schmitt, J., Krohne, G., 2004. Two novel LEM domain proteins are splice products of the annotated *Drosophila melanogaster* gene CG9424 (Bocksbeutel). Eur. J. Cell. Biol. 82, 605–616.

Wagner, N., Kagermeier, B., Loserth, S., Krohne, G., 2006. The *Drosophila melanogaster* LEM-domain protein MAN1. Eur. J. Cell. Biol. 85, 91–105.

Yu, K., Srinivasan, S., Shimmi, O., Biehs, B., Rashka, K.E., Kimelman, D., O'Connor, M.B., Bier, E., 2000. Processing of the *Drosophila* Sog protein creates a novel BMP inhibitory activity. Development 127, 2143–2154.

Zeng, Y.A., Rahnama, M., Wang, S., Sosu-Sedzorme, W., Verheyen, E.M., 2007. *Drosophila* Nemo antagonizes BMP signaling by phosphorylation of Mad and inhibition of its nuclear accumulation. Development 134, 2061–2071.